Journal of Physics: Conference Series

PAPER • OPEN ACCESS

Investigation of dropwise condensation of water through an efficient individual-based model

To cite this article: M Tancon *et al* 2024 *J. Phys.: Conf. Ser.* **2766** 012154

View the article online for updates and enhancements.

You may also like

- Relationships between economic development and resident environmental behavior and participation in areas with different economic and similar natural and cultural conditions
Junli Wu, Guijuan Gao, Bing Zhang et al.
- A double-walled carbon nanotubes conducting wire prepared by dip-coating
Chong Xie, Shenghui Yang, Jian-Wen Shi et al.
- First-order kinetics bottleneck during photoinduced ultrafast insulator–metal transition in 3D orbitally-driven Peierls insulator $CuIr_2S_4$
M Naseska, P Sutar, Y Vaskivskyi et al.

This content was downloaded from IP address 147.162.24.115 on 05/06/2024 at 07:51

Journal of Physics: Conference Series **2766** (2024) 012154 doi:10.1088/1742-6596/2766/1/012154

Investigation of dropwise condensation of water through an efficient individual-based model

M Tancon, A Abbatecola, M Mirafiori, S Bortolin and D Del Col
University of Padova, Department of Industrial Engineering
Via Venezia 1, 35131 – Padova, Italy
E-mail: stefano.bortolin@unipd.it

Abstract. In recent years, researchers have directed their studies towards solutions aimed at enhancing heat exchangers effectiveness. In this context, dropwise condensation (DWC) has been identified among the most promising solutions to increase the condensation heat transfer coefficient (HTC). In fact, DWC provides heat transfer coefficients up to ten times higher than those achievable during filmwise condensation (FWC), resulting in both economic and energy benefits. The DWC phenomenon is usually modelled by combining the heat exchanged through a single droplet and the drop-size distribution. The latter can be divided into a distribution of large droplets $N(r)$, determinable analytically by semi-empirical models, and a distribution of small droplets $n(r)$, typically determined through statistical approaches called population-based models. Another possibility for the determination of the droplet-size density is to simulate the DWC process by an individual-based model (IBM). In this case, each drop is tracked throughout its entire life cycle (nucleation, growth, coalescence, sliding), and the drop-size distribution is obtained as a result. In this paper, a new IBM for the simulation of DWC of steam is proposed. The developed model allows for the simulation of more than 10 million droplets while keeping an acceptable simulation time thanks to the implementation of parallel computing. The predictions obtained from the model, in terms of drop-size distribution and condensation heat flux, are compared against both PBM results and experimental data.

1. Introduction

Traditionally, filmwise condensation (FWC) has been the prevailing heat transfer mechanism encountered in industrial applications. However, by reducing the wettability of the subcooled wall, a more efficient condensation mechanism, known as dropwise condensation (DWC), can be achieved. Because the heat transfer coefficient (HTC) during DWC can be up to 10 times higher compared to FWC [1,2], heat exchangers can be significantly downsized or the driving temperature difference of the process can be reduced, leading to economic and energy savings.

DWC is a complex phenomenon involving mechanisms at different temporal and spatial scales. After nucleation, the drops grow by both direct condensation and coalescence until they reach the maximum size (departing radius) and then slide along the surface, exposing new nucleation sites. Due to the current limitations of optical systems, precise investigation of the small droplet population ($r < \sim 1$ μm) is very difficult, especially in the case of saturated conditions and high heat fluxes [3]. To overcome these issues, computational modeling offers a powerful tool for understanding DWC.

Usually, the DWC heat flux is evaluated by coupling a model for the calculation of the heat transfer through a single drop with a drop-size density function [4] (population-based models, PBMs). Single drop heat transfer models are based on the resolution of a network of thermal resistances. For drop-size

Content from this work may be used under the terms of the Creative Commons Attribution 4.0 licence. Any further distribution of this work must maintain attribution to the author(s) and the title of the work, journal citation and DOI.
Published under licence by IOP Publishing Ltd

distribution, the Le Fevre and Rose [5] model is commonly used to describe the distribution of large drops, while the small drops distribution is determined from the population balance theory. Individual-based models (IBMs) allow to evaluate the drop-size distribution by simulating the growth of each droplet [6]. While IBMs have been widely applied in the case of superhydrophobic surfaces, modeling of DWC on hydrophilic and hydrophobic surfaces has been marginally addressed due to the high computational cost when simulating large numbers of drops. In fact, when considering hydrophilic surfaces, the nucleation site density is expected to be higher compared to the case of superhydrophobic surfaces and also the droplets departing diameter becomes larger, thus requiring an extension of the computational domain.

In the present work, a new efficient IBM to simulate DWC of steam is presented. Using parallel computing, the developed model allows to simulate more than 10^7 drops in the domain. Then, the main results of the present IBM are discussed and compared against predictions by a PBM and against experimental data obtained on a nearly hydrophobic surface (advancing contact angle 87°).

2. Numerical simulations

2.1. Overview of the numerical method (IBM)

As a first step, nucleation sites are randomly distributed on the computational domain according to Poisson distribution. Then, a drop with size equal to the smallest thermodynamically viable radius (r_{min}) is placed on each nucleation site. During the simulation, the droplets grow, coalesce and slide, cleaning the surface and thus making available new nucleation sites. The developed model introduces innovative features that differentiate it from existing IBMs. Employing a hybrid approach that integrates MATLAB® and C programming languages, the present IBM uses the OpenMP library to distribute the computational load across all available CPU cores, significantly enhancing its computational efficiency. Moreover, unlike most models in the literature, the present IBM can consider a non-zero droplet acceleration. The machine used for the simulations is equipped with 128 GB of RAM and an AMD EPYC™ 7282 16C/32T CPU.

Table 1. Input data for numerical simulations

Coatings characteristics	Value	Thermodynamic conditions	Value
Advancing contact angle, θ_a [°]	87	Saturation temperature, T_{sat} [°C]	108
Receding contact angle, θ_r [°]	67	Subcooling degree, ΔT [K]	3.5
Thickness, δ_{HC} [nm]	380	Vapor velocity, v_v [m s^{-1}]	13.8
Thermal conductivity λ_{HC} [W m^{-1} K^{-1}]	0.25		

Two types of inputs are required by the present IBM: physical and numerical inputs. Physical input are reported in Table 1, while numerical input include the time step between two iterations ($\Delta\tau$), the nucleation sites density (N_s) and the computational domain area. For this study, the simulations were performed considering N_s values from 10^9 to 5×10^{12} m^{-2} and a computational domain of 1.5×1.5 mm^2. In general, a high time step results in shorter computational time but lower accuracy in tracking the growth of small drops, which in turn affects the drop-size density function and the calculated heat flux. According to the analyses discussed in Mirafiori *et al*. [6], a time step of 10^{-5} s has been chosen to correctly describe the evolution of the droplet population. A further input needed by the IBM is the model of heat transfer through a single drop.

The outcomes are the time-averaged drop-size distribution, the instantaneous and average heat flux. The drop-size distribution is calculated by dividing the range of droplet radii from r_{min} (minimum radius) to r_{max} (departing radius) into different bins and counting the number of droplets whose radius falls within each bin. Instead, the instantaneous heat flux is calculated as the sum of the heat transferred by each droplet on the surface. The simulations end when a quasi-steady state is achieved, characterized by instantaneous heat flux variations that consistently fall within 1% of the average heat flux.

2.2. Modelling of droplets growth, coalescence and sliding

The droplet growth rate due to vapor condensation is calculated by applying a model for the heat transfer through the drop. The Lethuillier *et al*. [7] model is here employed, as it offers the widest validity range of contact angles (20°-170°) and Biot number (10^{-4}-10^{5}). According to this model, the heat transfer rate through a single drop (Q_d) is given by:

$$Q_d = \left[\pi r^2 \left(1 - \frac{r_{min}}{r} \right) \Delta T \right] \Bigg/ \left(\frac{\delta_{HC}}{\lambda_{HC} \sin^2 \theta_e} + \frac{1}{2h_i \left(1 - \cos \theta_e \right)} + \frac{\pi r}{\lambda_l} f \right) \tag{1}$$

where θ_e is the equilibrium contact angle. For the analytical expressions of coefficients h_i and f the reader can refer to the manuscript by Lethuillier *et al*. [7].

In the case of a hydrophilic surface ($\theta < 90°$), the coalescence occurs when the distance between the centre of mass of the involved droplets becomes smaller than the sum of their base radii. A new droplet is then instantaneously placed at the centre of mass of the involved droplets, and its radius is determined considering the volume conservation. After a coalescence event, the availability of nucleation sites is evaluated and a drop with radius r_{min} is located at each unoccupied site.

Finally, when the droplet achieves the calculated departure dimension, the sliding process takes place. In the present IBM, the updated model by Tancon *et al*. [8] was implemented to evaluate r_{max} in the presence of a non-negligible vapor velocity. A novelty introduced by the present IBM is related to the sliding velocity, which is no longer considered at fixed velocity. In fact, the droplets motion during DWC is considered uniformly accelerated and the movement direction depends on the coalescences that occur during sliding. Further details on the developed IBM can be found in Mirafiori *et al*. [6].

3. Results and discussions

In Sec. 3.1, a comparison between the present IBM and the predictions obtained from a selected PBM is presented. In Sec. 3.2, the present IBM results are compared in terms of drop-size distribution and heat flux against the experimental data obtained by Tancon *et al*. [9].

3.1. Droplet population and heat flux: PBM vs IBM

As well established in the literature regarding PBMs, once the heat transferred through a single drop and the average drop-size distribution are known, the total heat flux during DWC can be calculated as:

$$q = \int_{r_{min}}^{r_e} Q_d(r) n(r) \mathrm{d}r + \int_{r_e}^{r_{max}} Q_d(r) N(r) \mathrm{d}r \tag{2}$$

In equation (2), $n(r)$ is the drop-size density of small droplets, growing by direct condensation, $N(r)$ is the drop-size density of large droplets, growing mainly by coalescence, and r_e is the effective radius, which can be expressed as $r_e = (4\, N_s^{0.5})^{-1}$.

The semiempirical law proposed by Le Fevre and Rose [5] is commonly used to describe $N(r)$ as:

$$N(r) = \frac{1}{3\pi\, r_{max}\, r^2} \left(\frac{r}{r_{max}} \right)^{-2/3} \tag{3}$$

For a fixed departing radius, $N(r)$ is only function of droplet radius r.

Based on the conservation of the number of droplets within a certain size range, the population balance theory can be solved to determine $n(r)$. This solution leads to a differential equation that can be analytically solved, yielding to the following general expression:

$$n(r) = N(r_e) \frac{r \left(r_e - r_{min} \right) \left(A_2 r + A_3 \right)}{r_e \left(r - r_{min} \right) \left(A_2 r_e + A_3 \right)} e^{B_1 + B_2} \tag{4}$$

where the coefficients A_2, A_3, B_1 and B_2 depends on the model used for the calculation of the heat transfer through a single drop. In this work, the coefficients found by Miljkovic *et al*. [10] are considered.

Figure 1a shows the overall heat flux obtained by the present IBM together with the one calculated by a PBM solved considering equation (3) for the large droplet population, equation (4) with the coefficients by Miljkovic *et al*. [10] for the small droplet population and equation (1) for the heat flux transferred by a single drop. Both the simulations and the PBM calculations were run under the conditions listed in table 1 using the following numerical parameters: $A = 1.5 \times 1.5$ mm^2, $r_{max} = 0.7$ mm, and $\Delta\tau = 10^{-5}$ s. The heat flux increases with the nucleation sites density for both the models (figure 1a). Nevertheless, the IBM exhibits an almost linear trend for the range of investigated N_s (limited to $N_s = 5 \times 10^{12}$ m^{-2}). The heat flux predicted by the PBM follows a curve with two different slopes. The PBM gives higher heat flux predictions than the IBM, with a minimum deviation with respect to the IBM of 30% at $N_s = 5\ 10^{12}$ m^{-2} and a maximum deviation of 53% at $N_s = 10^9$ m^{-2}.

This difference in the estimated heat flux can be attributed to the droplet population predicted by the two models. In figure 1b, the drop-size distribution obtained by PBM and IBM are compared at fixed nucleation site density ($N_s = 10^9$ m^{-2}). The graph shows that the present IBM predicts a different distribution of small drops compared to the PBM. Since drops with a radius close to r_e are responsible for most of the heat flux exchanged during DWC, an overestimation of their number leads to a significant overestimation of the total heat flux (figure 1a).

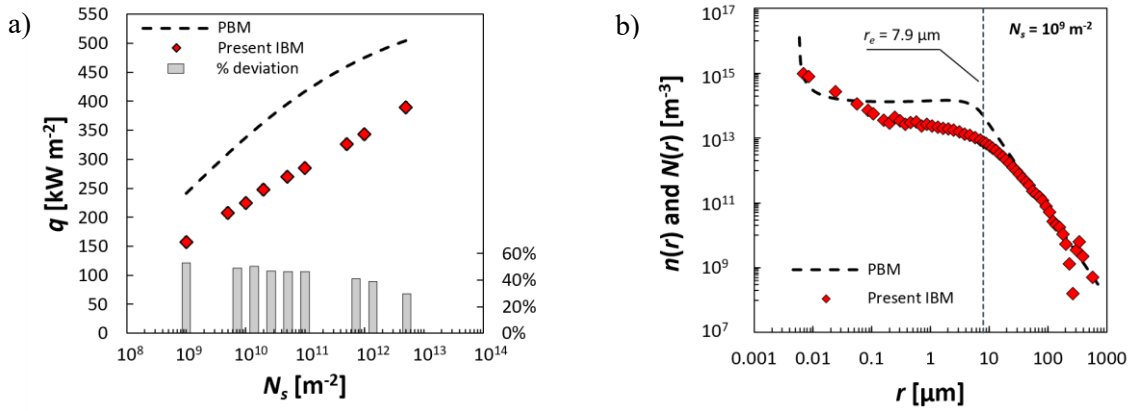

Figure 1. Numerical results obtained with the present IBM compared against PBM predicted values: a) average heat flux plotted versus nucleation sites density and b) drop-size distribution versus droplet radius.

3.2. Comparison with experimental data

A comparison with experimental data is here performed in terms of droplet population and heat flux. Measurements are taken from Tancon *et al*. [9] and refer to $v_v = 13.8$ m s^{-1}, $T_{sat} = 107$ °C and $q = 405$ kW m^{-2}, while simulations were performed using the inputs reported in table 1, with $\Delta\tau = 10^{-5}$ s and $N_s = 5 \times 10^{12}$ m^{-2}. The latter was chosen to match the experimental heat flux and the reliability of the chosen value was then checked from the observation of droplet growth rate.

In figure 2a, the measured drop-size distribution is compared against that predicted by the present IBM. For comparison, the distribution of large drops given by Le Fevre and Rose [5] and the small droplet distribution calculated according to Miljkovic *et al*. [10] are also depicted. The DWC visualization performed by a high-speed camera combined with a 12x zoom lens allows to map the population of large droplets with radii down to about 10 µm. Thus, by using the present optical technique, it is not possible to experimentally evaluate the left part of the drop-size distribution of large drops $N(r)$ and the entire small droplet distribution $n(r)$. As shown in figure 2a, the drop-size distributions obtained from both the numerical and experimental approach are in good agreement with the PBM model within the range of droplet radii from 10 µm to $r_{max} = 0.7$ mm. The present IBM allows the identification of three distinct zones of the drop-size density function. The first zone corresponds to the smallest droplets (with radii from r_{min} to 0.04 µm), which grow mainly by direct condensation of vapor. The third zone is related to the largest drops (with radii from 0.3 µm to r_{max}) growing mainly by

coalescence. In the second zone (droplets with radii from 0.04 μm to 0.3 μm), the two growth mechanisms interact with each other. This intermediate zone is neglected by the PBMs since the resolution of the population balance theory assumes a single value of radius (r_e) as the threshold between the two growth mechanisms.

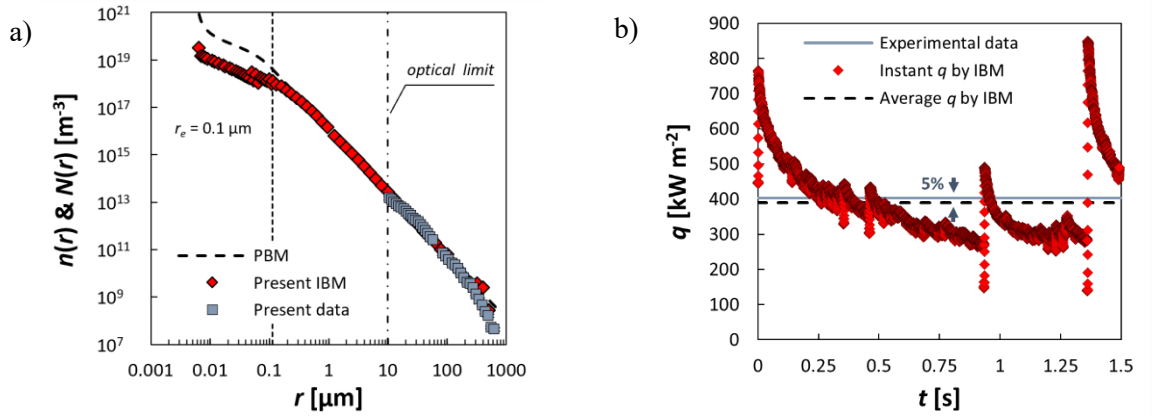

Figure 2. a) Experimental drop-size distribution compared with those predicted by the present IBM and by a PBM. b) Instant and average heat flux predicted by the IBM compared with the experimental measured value equal to 403 ± 15 kW m^{-2}.

Figure 2b shows the instant heat flux evaluated by the IBM during a 1.5 s time interval of DWC, in which one sliding event occurs. When large drops cover the surface, the heat flux is at the minimum value (about 130 kW m^{-2}) because the thermal resistance due to conduction inside the drops is high; immediately after the droplet sliding at 1.36 s, the conduction resistance through the drop becomes negligible, causing a rapid increase in the heat flux up to 800 kW m^{-2}. The instantaneous heat flux has an almost cyclic behaviour after this sliding event. As shown in figure 2b, the average heat flux calculated by the IBM is in good agreement with the experimental data (403 kW m^{-2}), with a deviation between the numerical and experimental value of 5 %.

To check if the experimental growth rate is well-approximated by the present IBM, figure 3 shows a comparison between the experimental and numerical evolution of drop dimensions over time. The initial time of the comparison (t = 0 s) is identified by matching two images with a similar drop-size distribution, one from the video and the other from simulations. The droplet growth rate is then analyzed for both cases at two different time instants.

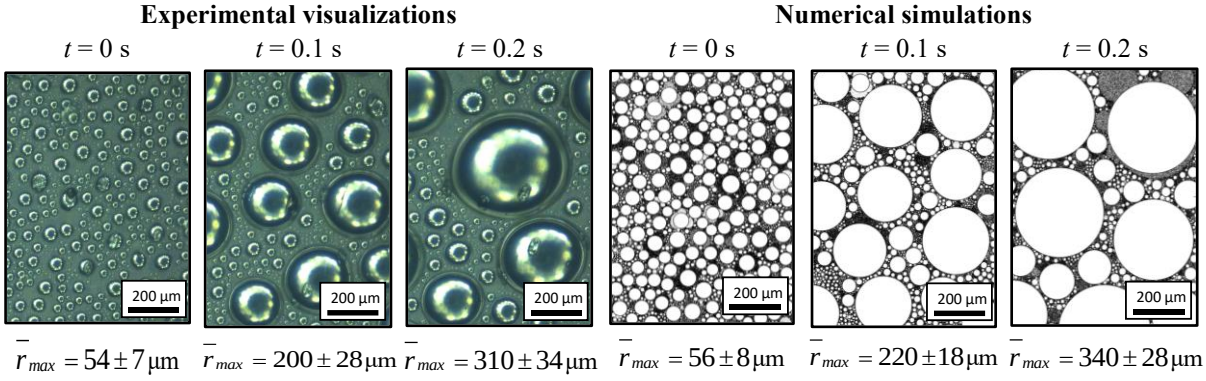

Figure 3. Comparison between experimental data and simulation results looking at the temporal evolution of droplets' dimensions at three different time steps t (0 s, 0.1 s, and 0.2 s).

After 0.1 s, the average radius of the larger drops detected in the real video is 200 ± 28 μm, while in the simulation is about 220 μm. After 0.2 s, droplets dimensions increased in both cases, without showing a significant discrepancy: the average radius of the larger drops observed in the experimental video is 310 ± 34 μm, while for the simulation is about 340 μm. Hence, it is possible to conclude that the present IBM is able to follow the temporal evolution of droplets dimensions (growth rate) evaluated by experimental visualization, with an average deviation between experimental and numerical values lower than 10%.

4. Conclusions

A new individual based model (IBM) implemented in a hybrid MATLAB® and C programming languages solution is here presented. The IBM results are compared against predictions from a population-based model (PBM) available in the literature and against experimental data. The comparison between the present IBM and the population-based model shows that the PBM overestimates the heat flux from 30% to 53%, depending on N_s. This is due to the calculation of the distribution for the small droplet population. Capable of simulating over 10 million droplets, present IBM allows a direct comparison of its results against experimental data obtained during steam DWC. The results of present IBM coupled with the Lethuillier *et al*. [7] model for the calculation of the single droplet heat transfer are compared in terms of drop-size distribution and heat flux against experimental data measured by Tancon *et al*. [9] at T_{sat} = 107 °C and q = 405 kW m^{-2}. For drop radii between 10 μm and r_{max}, the experimental data are in excellent agreement with the simulated drop-size distribution, following the power law proposed by Le Fevre and Rose [5]. It was found that the mean heat flux predicted by the IBM deviates by only 5 % from the experimental value. Furthermore, comparing the sequence of images obtained from high-speed video recordings with the simulations, it is possible to conclude that the present IBM is also able to accurately predict the growth rate for large droplets.

Acknowledgments

Financial support of European Union - Next Generation EU and Italian Ministry for University and Research (MUR) through the project PRIN 2022 (2022PSPA8R) WADERE is gratefully acknowledged.

References

[1] Basso M, Colusso E, Tancon M, Bortolin S, Mirafiori M, Guglielmi M, Del Col D and Martucci A 2023 *J. Non-Crystalline Solids X* **17** 100143
[2] Bortolin S, Tancon M and Del Col D 2022 *Surf. Wettability Eff. Phase Chang.* 29–67
[3] Parin R, Tancon M, Mirafiori M, Bortolin S, Moro L, Zago L, Carraro F, Martucci A and Del Col D 2020 *Appl. Therm. Eng.* **179** 115718
[4] Tancon M, Parin R, Bortolin S, Martucci A and Del Col D 2021 *Int. J. Heat Mass Transf.* **165** 120624
[5] Le Fevre E J and Rose J W 1966 *Proceedings of the 3rd International Heat Transfer Conference, Volume 2*
[6] Mirafiori M, Tancon M, Bortolin S and Col D Del 2024 *Int. J. Heat Mass Transf.* **222** 125109
[7] Lethuillier J, Miscevic M, Lavieille P, Blanco S, Coustet C and Topin F 2022 *Appl. Therm. Eng.* **209** 118233
[8] Tancon M, Abbatecola A, Mirafiori M, Bortolin S, Colusso E, Martucci A and Del Col D 2024 *Int. J. Therm. Sci.* **196** 108738
[9] Tancon M, Mirafiori M, Bortolin S, Basso M, Colusso E and Del Col D 2022 *Appl. Therm. Eng.* **216** 119021
[10] Miljkovic N, Enright R and Wang E N 2013 Modeling and Optimization of Superhydrophobic Condensation *J. Heat Transfer* **135** 111004